Room temperature iron-catalyzed transfer hydrogenation and regioselective deuteration of carbon-carbon double bonds

Maialen Espinal-Viguri,[§‡] Samuel E. Neale,[†] Nathan T. Coles,[§‡] Stuart A. Macgregor[*†] and Ruth L. Webster[*§]

§Department of Chemistry, University of Bath, Claverton Down, Bath, United Kingdom, BA2 7AY.

†Institute of Chemical Sciences, Heriot-Watt University, Edinburgh, United Kingdom, EH14 4AS.

ABSTRACT: An iron catalyst has been developed for the transfer hydrogenation of carbon-carbon multiple bonds. Using a well-defined β-diketiminate iron(II) pre-catalyst, a sacrificial amine and a borane, even simple, unactivated alkenes such as 1-hexene undergo hydrogenation within 1 hour at room temperature. Tuning the reagent stoichiometry allows for semi- and complete hydrogenation of terminal alkynes. It is also possible to hydrogenate amino-alkenes and amino-alkynes without poisoning the catalyst through competitive amine ligation. Furthermore, by exploiting the separate protic and hydridic nature of the reagents it is possible to regioselectively prepare mono-isotopically labeled products. DFT calculations define a mechanism for the transfer hydrogenation of propene with $^{n}BuNH_2$ and HBpin that involves the initial formation of an iron(II)-hydride active species, 1,2-insertion of propene and rate-limiting protonolysis of the resultant alkyl by the amine N-H bond. This mechanism is fully consistent with the selective deuteration studies, although the calculations also highlight alkene hydroboration and amine-borane dehydrocoupling as competitive processes. This was resolved by re-assessing the nature of the active transfer hydrogenation agent: experimentally a gel is observed in catalysis and calculations suggest this can be formulated as an oligomeric species comprising H-bonded amine-borane adducts. Gel formation serves to reduce the effective concentrations of free HBpin and $^{n}BuNH_2$ and so disfavors both hydroboration and dehydrocoupling while allowing alkene migratory insertion (and hence transfer hydrogenation) to dominate.

1. Introduction

Transfer hydrogenation is well explored using metal catalysis; classic examples include the Meerwein-Ponndorf-Verley reduction using an aluminium alkoxide[1] and use of Shvo's Ru-hydride complex[2] or the chiral Noyori Ru-based catalyst for enantioselective transfer hydrogenation.[3] Very often these reactions reduce a carbonyl compound using a simple sacrificial alcohol. In contrast, using an amine and a borane as the transfer hydrogenation agents is less common. In this regard, most reactions rely on dehydrogenation of the amine and borane to release H_2, which then undertakes the reduction. Hydrogenations of this type with homogeneous Zr, Cr, Re, Ru, Co, Rh, Ni, Pd and Cu catalysts, Frustrated Lewis Pairs and borate organocatalysts are known for the reduction of alkenes, alkynes, imines, nitriles, nitro groups, aldehydes and ketones.[4]

It is important to note that the reduction of unsaturated bonds by an amine and borane that makes direct use of their separate protic and hydridic natures is not common. Berke and co-workers have exploited the highly polarized nature of vinyl malononitriles[5] or imines[6] to transfer H^+ and H^- from ammonia-borane. They are able to deuterate $C^{\delta+}$ selectively when employing $NH_3{\cdot}BD_3$ and $N/C^{\delta-}$ when employing $ND_3{\cdot}BH_3$. Although catalyst-free, this reaction is limited to highly polarized unsaturated systems and deuteration has only been explored with one imine (*N*-benzylidene aniline) and one malononitrile substrate (2-cyclohexylidenemalononitrile). Building on the work of Berke, Yang and Du used a chiral phosphoric acid in the presence of ammonia-borane to undertake enantioselective imine transfer hydrogenation[7] and Braunschweig has undertaken transfer hydrogenation of iminoboranes using $NH_3{\cdot}BD_3$ and $ND_3{\cdot}BH_3$.[8] Metal-catalyzed examples include Westcott's report using 5 mol% Wilkinson's catalyst, 1.1 equivalent HBcat and 4-vinylaniline, where the double bond is reduced and the *N*,*N*-diborylated product is obtained.[9] Luo and Liu's Co-catalyzed *Z*- and *E*-selective semi-hydrogenation of alkynes[10] uses $NH_3{\cdot}BH_3$ as the hydride source but in this case MeOH or EtOH act as the proton source. More recently El-Sepelgy reported an Mn-pincer complex for the semi-hydrogenation of alkynes with a computed catalytic cycle that implies separate proton and hydride transfer events,[11] whilst Driess used an Mn-silylene system for a similar series of transformations.[12]

Catalysis that proceeds *via* σ-bond metathesis offers the ideal opportunity to exploit the combined protic/hydridic nature of amines and boranes for the reduction of unactivated, non-polarized double bonds and to regioselectively install deuterium. Unlike standard transfer hydrogenation reactions which often rely on an alcohol as the sole proton and hydride source, this alternative method allows for more facile discrimination between positions on the double bond, particularly when employing simple alkene substrates.

We have previously demonstrated the ability of the iron β-diketiminate moiety to effect catalytic alkene hydroboration,[13] hydrophosphination[14] and amine-borane dehydrocoupling reactions.[15] Here we hypothesized that if we could access a catalytic cycle that exploited iron β-diketiminate's innate ability to facilitate both hydride transfer and protonation reactions *via* σ-bond metathesis (Scheme 1), we should be able to hydrogenate unactivated alkenes using an amine and a borane: an unprecedented transformation in iron catalyzed hydrogenation chemistry. It is worth noting that several examples of iron-catalyzed hydrogenation using H_2 have been reported, including the reduction of carbonyls, alkenes, alkynes, nitro groups and α,β-unsaturated systems with H_2 pressures ranging from

1 to 30 bar.[16] Important to note is Wolf and von Wangelin's use of an Fe(I) β-diketiminate dimer, which fails to show any activity for the hydrogenation of styrene using 2 bar H_2;[17] indicating that we are able to access a different reaction mechanism from that of low oxidation state Fe catalysis. To the best of our knowledge only two examples exist where more challenging substrates, *e.g.* a primary amino-alkene[18] or hydroxy-alkene,[19] have been hydrogenated, although both were in poor yield (20% and 10% respectively). There are also only limited examples of iron-catalyzed transfer hydrogenations[20] that tackle simple C-C *sp* or sp^2 bonds[21]: most examples focus on carbonyls[22] or α,β-unsaturated systems.[23]

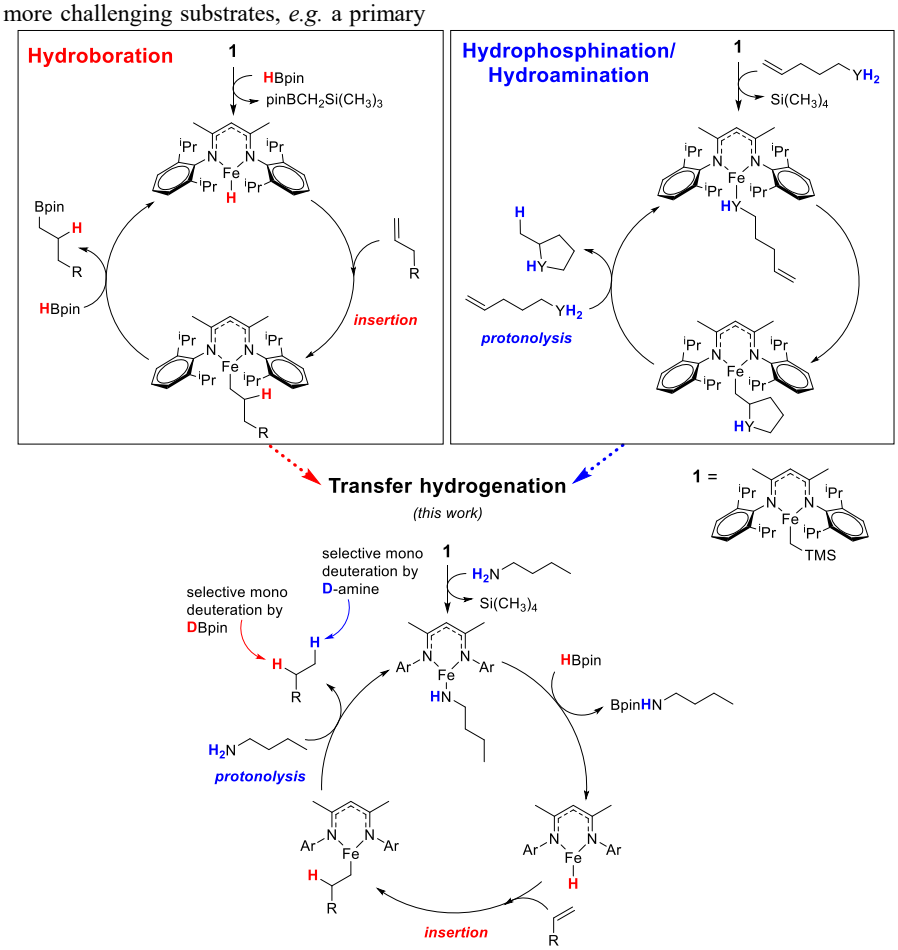

Scheme 1. A hypothetical transfer hydrogenation process based on mechanistic understanding of hydroboration[13] and hydrophosphination[14a]/hydroamination.[24]

2. Substrate Scope

Following a short optimization procedure, we found that a primary amine is the optimum source of protons; to avoid any steric issues we decided to use $^nBuNH_2$ as an inexpensive, sacrificial proton source. Reactions using secondary amines proceed but result in a significantly poorer yield of product. HBpin is the best source of hydride. Reaction progress can be monitored visually: instantaneous gelation occurs when the final reagent (HBpin) is added to the mixture (see ESI). This dissipates as the reactions proceed and the solution returns to its original viscosity when complete. We started by testing transfer hydrogenation across a range of different unsaturated systems (Table 1). The majority of reactions are complete within minutes at room temperature using 10 mol% **1** but were left for 1 hour to ensure maximum conversion for all substrates.[25] There is no reaction in the absence of **1** whilst an excess of HBpin leads to competitive hydroboration and amine-borane dehydrocoupling, supporting our computational studies (see Section 3 and ESI).

Table 1. Transfer hydrogenation substrate scope using $^nBuNH_2$ and HBpin.

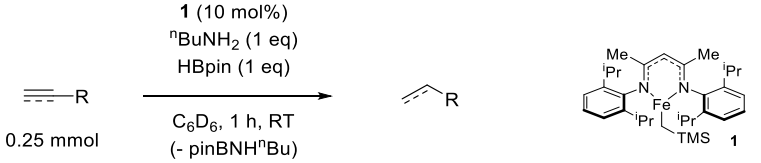

Entry	Starting Material	Product		Yield (%)[a]
1	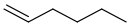		2a	91
2	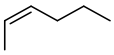		2a	(28)
3	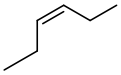		2a	(48)
4	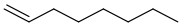		2b	88
5	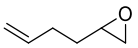	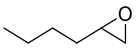	2c	**91**
6			2d	**81**
7[b]	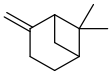	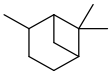	2e	(46)
8[c]	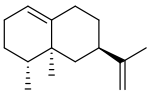	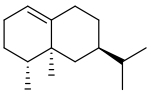	2f	80
	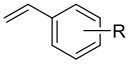	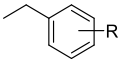		
9[d]	R =	H	2g	45
10		4-Me	2h	62
11		4-OMe	2i	**77**
12		4-CF_3	2j	**65**
13		4-Cl	2k	(65)
14		4-Br	2l	(38)
15		3-Br	2m	(80)
16		4-Ph	2n	**100**
17[e]	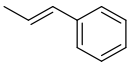	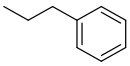	2d	**99**
18[f]	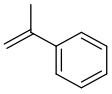	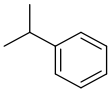	2o	**98**
19		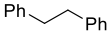	2p	**97**
20			2q	95
21[g]		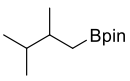	2r	**57**
22[h]	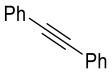	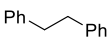	2p	**68**
23[i]			2s	46
24[j]			2g	68

25[i]	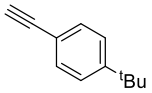	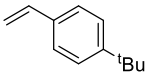	2t	**45**

Reaction conditions: all reactions performed in a J-Young NMR tube. 0.25 mmol alkene/alkyne, 0.25 mmol $^{n}BuNH_2$, 0.25 mmol HBpin, 10 mol% **1**, 0.5 mL C_6D_6, 1 h, RT. [a]All reactions give 100% conversion to product with the exception of results in parentheses (also see Ref 25). Conversion to product is based on uptake of starting material. Yields in bold are isolated yield. Other yields are spectroscopic in the presence of an internal standard whereby the product was not separated from C_6D_6: loss of product occurred during isolation (vacuum distillation of product and solvent). [b]18 h, 60 °C, 0.25 mmol aniline (no $H_2{}^{n}Bu$ used). [c]18 h, 90 °C, 0.25 mmol aniline (no $^{n}BuNH_2$ used). [d]6.5 h, RT. [e]16 h, RT. [f]4 h, 90 °C. [g]0.5 mmol HBpin, 0.25 mmol $^{n}BuNH_2$, 4 h, 90 °C. [h]0.5 mmol HBpin, 0.5 mmol $^{n}BuNH_2$, 16 h, 90 °C. [i]0.125 mmol $H_2N^{n}Bu$, 0.125 mmol HBpin: maximum yield of product is 50%. [j]0.5 mmol $H_2N^{n}Bu$, 0.5 mmol HBpin, 2 h.

The reaction tolerates aliphatic alkenes and functional groups such as epoxides (**2c**, Entry 5) along with electron donating (**2i**, Entry 11), electron withdrawing (**2j**, Entry 12) and halo-substituted (Entries 13, 14, 15) styrenes. More challenging terpene natural products can also be hydrogenated. β-Pinene is reduced at 60 °C without any evidence for isomerization to α-pinene (Entry 7). The exo-double bond of valencene is selectively reduced over the endo-double bond (Entry 8). Other internal alkene substrates such as *trans*-β-methylstyrene (Entry 17) proceed more slowly requiring 16 h at RT to go to completion, while α-methylstyrene (Entry 18) requires heating to 90 °C for 4 h for complete conversion. 2,3-Dimethylbuta-1,3-diene can be mono-hydrogenated selectively to form 2,3-dimethylbut-1-ene (**2q**, Entry 20) or an extra equivalent of HBpin can be added for dual functionalization to give (2,3-dimethylbutyl)pinacolborane (**2r**, Entry 21). Diphenylacetylene does not stop cleanly at stilbene and therefore two equivalents of amine and HBpin are needed to generate 1,2-diphenylethane (**2p**, Entry 22). Terminal acetylenes yield the styrene product when using HBpin and $^{n}BuNH_2$ as limiting reagents (**2s** and **2t**, Entries 23 and 25), or two equivalents of amine and borane yield ethylbenzene (Entry 24). The reaction is also amenable to scale-up with 82% **2d** obtained after 8 h at RT from the hydrogenation of 5 mmol allyl benzene with the catalyst loading scaled down to 0.5 mol% and aniline as the proton source.

Based on our hypothetical catalytic cycle (Scheme 1), it should be possible to hydrogenate aminoalkenes and aminoalkynes without the presence of sacrificial $^{n}BuNH_2$.[9] This would also demonstrate a much greater level of functional group tolerance than that reported using other iron-catalyzed hydrogenation methodologies,[18-19] where competing coordination of nucleophilic substituents is often detrimental to catalysis. This is indeed the case and a wide range of amine-containing alkenes and alkynes are tolerated (Table 2). Once again, hydrogenation is complete within minutes at room temperature and the nitrogen-boron bond that forms is readily cleaved during work-up, allowing the isolation of the primary aliphatic amine product in high yield.

Table 2. Transfer hydrogenation of aminoalkenes and aminoalkynes.

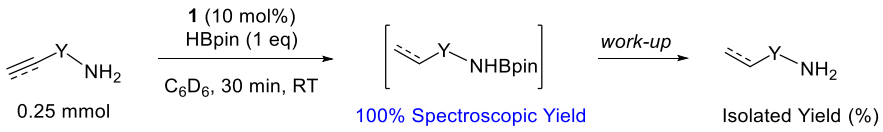

Entry	Starting Material	Product		Isolated Yield (%)
1	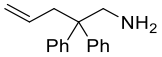	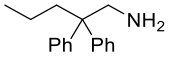	3a	92
2	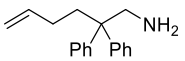	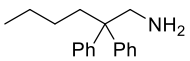	3b	89
3	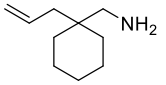	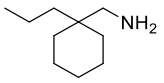	3c	80
4	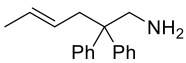	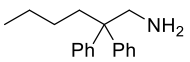	3b	95
5	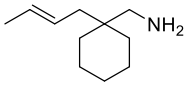	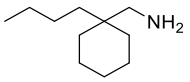	3d	71
6	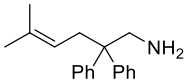	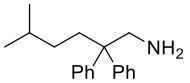	3e	94
7[a]	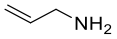	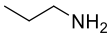	3f	-

8	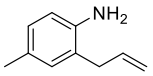	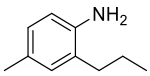	3g	86
9	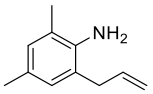	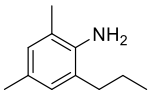	3h	88
10	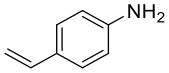	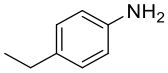	3i	82
11	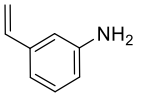	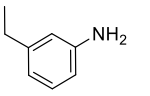	3j	89
12[b]	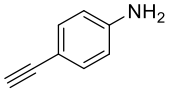	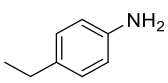	3i	50
13[b]	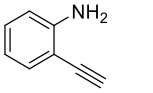	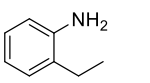	3k	74
14[c]	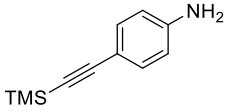	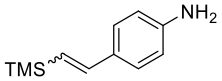	3l	90
15	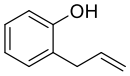	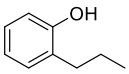	4a	82
16[a]	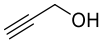	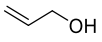	4b	-

Reaction conditions: all reactions performed in a J-Young NMR tube. 0.25 mmol alkene, 0.25 mmol HBpin, 10 mol% **1**, 0.5 mL C_6D_6, 30 min, RT. All spectroscopic yields are 100%. [a]Not isolated due to volatility, 100% spectroscopic yield based on formation of N–B or O–B product (see ESI). [b]0.5 mmol HBpin. [c]4 : 1 ratio of *trans* : *cis* products.

The system operates for internal aliphatic alkenes (Entries 4-6), with no observable reduction in rate of reaction, and for volatile substrates such as allyl amine (**3f**, Entry 7). Reduction of 2- and 4-ethynylaniline does not stop cleanly at the vinylaniline: two equivalents of HBpin are necessary to form the ethylaniline (**3i** and **3k**, Entries 12 and 13). Alcohols can also be used as the proton source, with 4-allylphenol (**4a**, Entry 15) and propargyl alcohol (**4b**, Entry 16) readily undergoing reduction at room temperature. Propargyl alcohol selectively generates allyl alcohol as the product; this is an intuitive result since there is only one proton per molecule of substrate. When used as a reagent, allyl alcohol cannot be hydrogenated to form propanol, presumably the slightly higher pK_a of this substrate prevents reactivity.

Isotopic labelling has also been carried out (Scheme 2). Based on our proposed catalytic cycle, an *N*,*N*-d_2-amine should lead to selective mono-deuteration at the terminal (anti-Markovnikov) position and DBpin should result in deuteration at the internal (Markovnikov) position of the double bond. If HD is released and undertakes the reduction there should be no regioselectivity. We can report that mono-deuteration of aliphatic alkenes is possible using *N*,*N*-d_2-aniline (Scheme 4a). Double deuteration is not observed. This is a rare example of selective catalytic mono-deuteration of a carbon-carbon double bond,[26] with most other examples in the literature furnishing deuteration across the double bond, simply because D_2 is necessary. For aliphatic substrates (**5a** to **5c**), discrimination between the positions on the double bond is largely dictated by sterics, unfortunately when styrenes are employed electronics begin to compete and there is a drop-off in selectivity for the terminal position (**5d** to **5f**). In fact there is a steady decrease in anti-Markovnikov selectivity moving from electron rich 4-OMe styrene (**5d**), through to styrene (**5e**) and finally almost complete erosion of selectivity when 4-CF_3 styrene (**5f**) is employed. A similar trend is observed when DBpin is used (Scheme 4b): aliphatic substrates (**6a** to **6c**) give good Markovnikov-selective mono-deuteration whereas 4-CF_3 styrene (**6f**) gives almost a 1:1 mixture of Markovnikov and anti-Markovnikov product. With the exception of **5h** and **6h**, substrates that have the potential to undergo double bond isomerization (e.g. **5a** to **5c**, **5g**, **6a** to **6c** and **6g**), deuterium incorporation at other positions in the molecule is not observed. The fact that deuteration of the α, β and γ carbon is observed for **5h** and **6h** suggests that a different mechanism, that involves isomerization, is at play. This is a facet of reactivity that we are currently investigating.

Scheme 2. a) Deuterium labelling occurs with good selectivity for functionalization of the terminal carbon when *N*,*N*-d_2-aniline is employed. b) DBpin results in a good level of selectivity for deuteration at the internal position of the double bond.

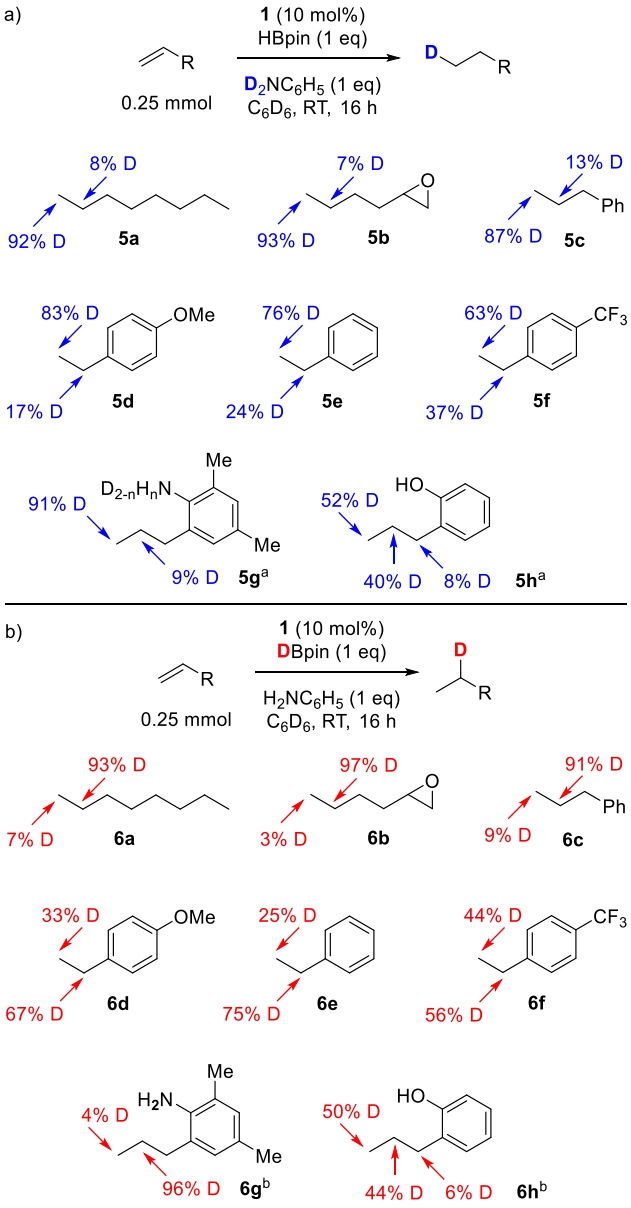

Reaction conditions: all reactions performed in a J-Young NMR tube. Results are an average of two runs. Left for 16 h to ensure complete conversion. 0.25 mmol alkene, 0.25 mmol amine, 0.25 mmol borane, 10 mol% 1, 0.5 mL C_6D_6, 16 h, RT. [a]*N,N-d*$_2$- or *O-d*$_1$-substrate (no aniline employed). [b]No aniline employed.

3. Computational studies

DFT studies were undertaken to model the transfer hydrogenation of propene as a simple model substrate using ^{n}BuNH$_2$ and HBpin and the full Fe β-diketiminate precursor, LFe–SiMe$_3$, **1** (denoted **I** in the computational study). Calculations employed the BP86 functional with an SDD pseudopotential and basis set on Fe and a standard double-ζ + polarization basis set on other atoms (BS1) for initial optimizations and free energy calculations. Energies were then recomputed with the B3PW91 functional including the effects of dispersion (D3 parameter set with Becke-Johnson damping), C_6H_6 solvent (PCM approach) and an extended def2tzvp basis set. This protocol resulted from benchmarking studies on β-H transfer in LFe–^{i}Bu for which experimental data have been reported by Holland and co-workers (see ESI).[27] Calculations also routinely assessed stationary points in both the quintet and the triplet spin-states, with the quintet usually being more stable: for example, ^{5}**I** (the quintet form of **I**) lies 19.4 kcal/mol below ^{3}**I** (the triplet form). Selected test calculations on singlet spin-states showed such species to be even higher in energy (see ESI). As reported previously by Holland and Cundari,[28] the triplet spin-state becomes energetically relevant for the alkene addition and migratory insertion steps.

3.1 Defining the nature for the transfer hydrogenation agent.

Our initial mechanistic hypothesis for transfer hydrogenation is set out in Scheme 1 and highlights the central role of an LFe–hydride species and its reaction with alkenes to form an LFe–alkyl. Both species can engage in a number of potentially competing processes, in particular, for LFe–alkyl protonolysis with amine is the proposed alkane release step in transfer hydrogenation, while reaction with HBpin would lead to hydroboration. Indeed, **1** has been shown to promote both the catalytic hydroboration of alkenes,[13] and the dehydrocoupling of amine-boranes.[15] An initial assessment of these processes was therefore undertaken at the LFe–^{n}Pr primary alkyl intermediate implicated in our model system, along with the related dehydrocoupling of ^{n}BuH$_2$N–BHpin that would also result in alkane formation along with H_2 release (see Scheme 3 and ESI for details).

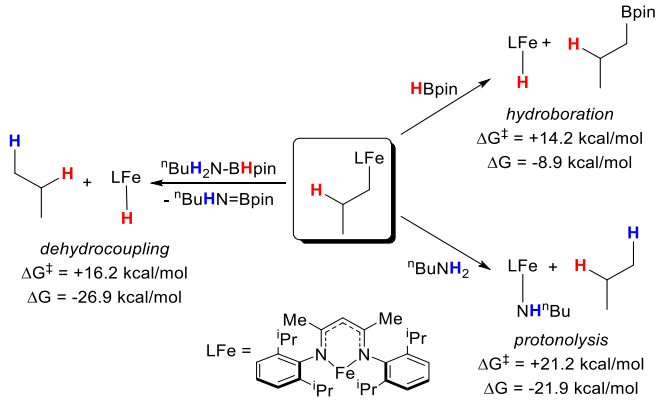

Scheme 3. Computed energetics (kcal/mol, B3PW91(D3-BJ,C_6H_6)/def2tzvp//BP86/BS1 level) for different competing reactions at LFe–^{n}Pr. Where several steps are involved $\Delta G^‡$ represents the total energy span, relative to LFe–^{n}Pr and the appropriate reactants.

The results in Scheme 3 show that, while all three processes are significantly exergonic, hydroboration to form ^{n}Pr–Bpin and LFe–H is most accessible kinetically with a barrier of 14.2 kcal/mol, 7.0 kcal/mol lower than that for protonolysis with ^{n}BuNH$_2$. This is consistent with alkene hydroboration reported in earlier studies;[13] however in the present context this result suggests that free HBpin cannot be present in solution. Instead the implication is that HBpin is sequestered in the presence of amine, for example by formation of

an amine-borane adduct, $^{n}BuH_2NBHpin$. Dehydrocoupling of $^{n}BuH_2NBHpin$ at LFe–^{n}Pr is also computed to be accessible, with a barrier of 16.2 kcal/mol^{-1}.

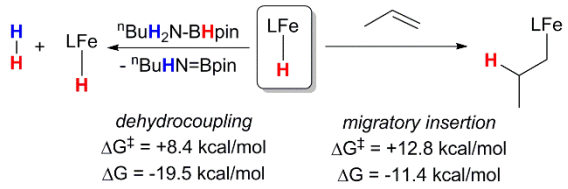

Scheme 4. Computed energetics (kcal/mol, B3PW91(D3-BJ,C_6H_6)/def2tzvp//BP86/BS1 level) for competing amine-borane dehydrocoupling and alkene insertion processes at LFe–H. Where several steps are involved $\Delta G^{‡}$ represents the total energy span, relative to LFe–H and the appropriate reactants. Migratory insertion involves a spin-crossover mechanism between the quintet and triplet surfaces - see text for details.

Having inferred the involvement of amine-borane adducts in the transfer hydrogenation process, we also found the dehydrocoupling of $^{n}BuH_2NBHpin$ at LFe–H to be very facile (Scheme 4). This is consistent with the room temperature dehydrocoupling of amine-boranes reported elsewhere.[15] However, dehydrocoupling was also computed to be more accessible than propene migratory insertion, implying that the former process should dominate to give amino-borane and H_2. In principle H_2 could then effect the alkene hydrogenation, but this would be inconsistent with the observed selectivity of transfer hydrogenation that clearly indicates free H_2 is not involved.[29]

To resolve these discrepancies we returned to a more detailed assessment of the nature of the "$^{n}BuH_2NBHpin$" adduct that is being formed in solution. As mentioned above, addition of HBpin to the reaction mixture results in the immediate formation of a thick, immiscible gel which only slowly dissolves as catalysis proceeds. A study by NMR spectroscopy gives some evidence for Lewis acid-base adduct formation. The ^{11}B NMR of 0.11 mmol HBpin in 0.5 mL THF displays a doublet at 28.4 ppm (J = 178.1 Hz). Addition of 0.1 mmol $H_2N^{n}Bu$ (no catalyst added) results in instantaneous gelation, complete loss of the HBpin signal and formation of a new doublet at 20.9 ppm (J = 160.5 Hz), indicating increased shielding of the boron nucleus by nitrogen, but without loss of B-H. This is consistent with Lewis acid-base adduct formation *e.g.* **AB1**, **AB2**, etc., see below. The gel resulted in significant line broadening of the ^{1}H NMR spectrum and therefore DOSY analysis to investigate molecular weight was not successful. After 24 h at room temperature, the gel disappears, the adduct signal is lost and a singlet associated with the dehydrocoupled product $^{n}BuHNBpin$ is observed at 24.7 ppm (Bertrand has shown that certain amines and boranes can dehydrocouple under catalyst-free conditions[30]) along with return of the HBpin doublet at 28.4 ppm (added in excess).

Given these observations, the accessibility of various [$^{n}BuH_2NBHpin$]$_n$ adducts was also assessed computationally (Figure 1). While formation of $^{n}BuH_2NBHpin$ (**AB1**) is computed to be endergonic by 3.1 kcal/mol, formation of dimeric and tetrameric H-bonded adducts **AB2** and **AB4** was found to be increasingly favored, with ΔG = +0.1 kcal/mol and -3.5 kcal/mol respectively.[31] These values also include a very large, negative, translational entropy which is known to be over-estimated in free energy calculations based on isolated molecules.[32] This indicates that the formation of oligomeric species, **ABn**, will be even more favorable than the computed values imply and so would be consistent with the presence of the gel seen experimentally. We therefore propose that oligomeric **ABn** is the active species in transfer hydrogenation in this case, and in the following mechanistic study we will model such a species with dimeric **AB2**.

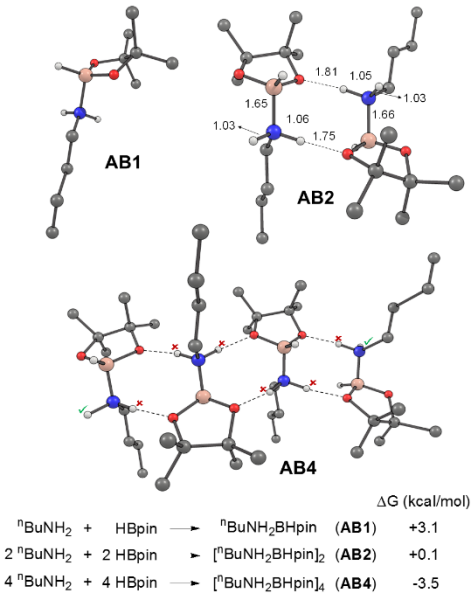

Figure 1. Computed structures and free energies of formation for amine-borane adducts [$^{n}BuH_2NBHpin$]$_n$ (n = 1, 2 and 4). Selected distances (in Å) are provided for **AB2** and these are representative of the metrics seen in the other adducts. For **AB4** free N-H protons on the edge of the tetramer are highlighted with a tick whereas those involved in intramolecular H-bonding are marked with a cross.

3.2 Mechanism of catalytic transfer hydrogenation.

Computed profiles for key steps in the transfer hydrogenation of propene with **AB2** mediated by catalyst ^{5}**I** are shown in Figure 2. Activation of ^{5}**I** is initiated by coordination of **AB2** via a B–H σ-interaction (Fe···H = 1.92 Å, B–H = 1.29 Å) to give the 4-coordinate adduct ^{5}**II** (+14.7 kcal/mol). Protonolysis of the Fe–alkyl bond then proceeds via ^{5}**TS(II-III)** at +22.4 kcal/mol to form 3-coordinate LFe–H, ^{5}**III**, with concomitant dehydrocoupling of one amine-borane unit within **AB2** to give **AB2$_{DHC}$** which features one amino- and one amine-borane moiety. ^{5}**III** is the active species in catalysis and incorporates a hydride ligand that is derived from HBpin. This initiation process has an overall barrier of 22.4 kcal/mol and is exergonic by 22.1 kcal/mol.

For the catalytic cycle we focus on the process based on 1,2-insertion to form the primary alkyl intermediate LFe-^{n}Pr. The issue of the regioselectivity of alkene insertion will be considered below.

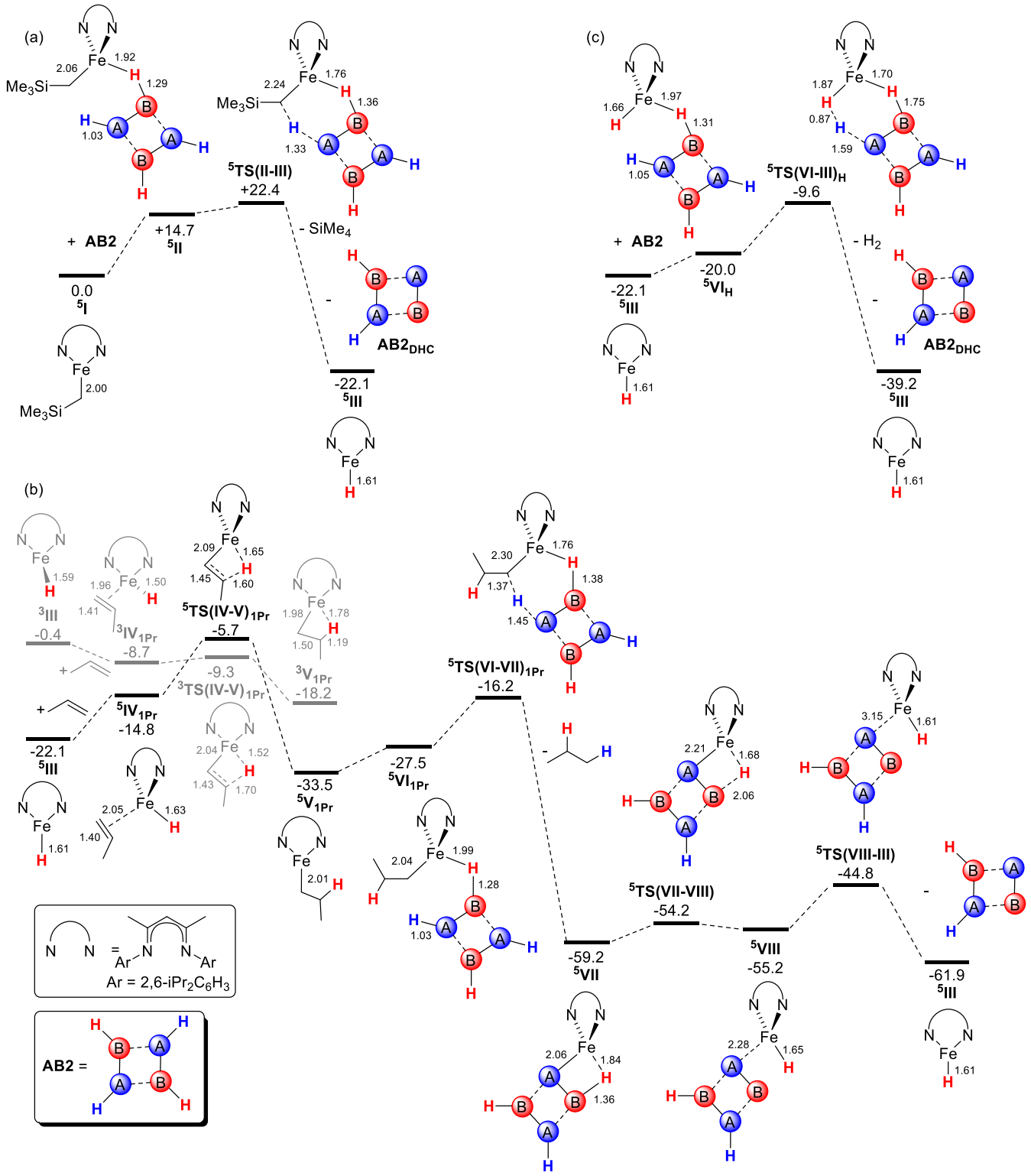

Figure 2. Computed free energy profiles (kcal/mol) for (a) the activation of pre-catalyst ^{5}**I** with **AB2**, (b) catalytic transfer hydrogenation of propene at ^{5}**III** with **AB2**, and (c) competing dehydrocoupling of **AB2** at ^{5}**III**. Data presented are for the quintet spin state except for alkene migratory insertion, where relevant triplet structures are also shown in grey. Selected distances are provided in Å.

Addition of propene to ^{5}**III** forms adduct ^{5}**IV$_{1Pr}$** from which migratory insertion can proceed on the quintet surface via ^{5}**TS(IV-V)$_{1Pr}$** at -5.7 kcal/mol. In this case, however, the equivalent triplet transition state, ^{3}**TS(IV-V)$_{1Pr}$**, is found to be more stable at -9.3 kcal/mol. Beyond this transition state the subsequent LFe-^{n}Pr intermediate reverts to the quintet state (^{5}**V$_{1Pr}$**, = -33.5 kcal/mol). A dual spin-crossover mechanism[33] is therefore in operation for the migratory insertion, which proceeds (assuming facile spin-crossover[34]) with an overall barrier, relative to ^{5}**III**, of 12.8 kcal/mol and ΔG = -11.4 kcal/mol. These findings are consistent with Holland and Cundari's study of similar alkene insertion processes.[28] Protonolysis of ^{5}**V$_{1Pr}$**

initially proceeds in a similar way to the activation of **^{5}I**, with coordination of **AB2** to form adduct **^{5}VI$_{1Pr}$** (-27.5 kcal/mol) and proton transfer via **^{5}TS(VI-VII)$_{1Pr}$** at -16.2 kcal/mol to release propane. In contrast to **^{5}I**, however, an amidoborate adduct, **^{5}VII**, is formed in this case (Fe–N = 2.06 Å) featuring a β-agostic interaction (Fe···H = 1.84 Å, B–H = 1.36 Å). β-H transfer via **^{5}TS(VII-VIII)** then yields **^{5}VIII**, in which **AB2$_{DHC}$** is bound through the amide nitrogen (Fe–N = 2.28 Å). Dissociation of **AB2$_{DHC}$** via **^{5}TS(VIII-III)** then reforms **^{5}III**.[35]

The three major processes along the catalytic cycle, migratory insertion, protonolysis and β-H elimination, have computed energy spans of 12.8 kcal/mol, 17.3 kcal/mol and 14.4 kcal/mol and this, along with the exergonicity of each step means that propane release via protonolysis of **^{5}VI$_{1Pr}$** through **^{5}TS(VI-VII)** is turnover-limiting. The modest barrier of 17.3 kcal/mol is consistent with efficient catalysis proceeding at room temperature. 1,2-insertion would also be consistent with the experimental labelling studies in that the hydride derived from HBpin adds to the internal carbon, while the proton derived from ^{n}BuNH$_2$ adds to the terminal carbon.

As noted previously, amine-borane dehydrocoupling at **^{5}III** can compete with alkene migratory insertion and so this process was also assessed with **AB2** (see Figure 2c). After formation of a B–H σ-bound adduct, **^{5}VI$_H$** (-20.0 kcal/mol), dehydrocoupling involves a concerted protonolysis of the Fe–H bond coupled to hydride transfer to Fe via **^{5}TS(VI-III)$_H$** (-9.6 kcal/mol) to afford H_2, **AB2$_{DHC}$** and **^{5}III**. The overall barrier for this process is 12.5 kcal/mol, close to that for the migratory insertion of propene ($\Delta G^‡$ = 12.8 kcal/mol). However, an additional consequence of the amine-borane oligomer formation is that the number of N-H protons available for reaction will be significantly reduced, with the majority being involved in intramolecular H-bonding. This is illustrated in Figure 1 for **AB4** where only 2 of the 8 protons are available due to their location on the edge of the aggregate (highlighted with a tick). With larger oligomers the proportion of free N-H bonds will drop further. Thus not only does adduct and oligomer formation remove free HBpin from solution (and so avoid hydroboration) it also has the effect of reducing the effective concentration of the amine, allowing the alkene migratory insertion (and thus transfer hydrogenation) to dominate.

3.3 Regioselectivity studies

The computed catalytic cycle in Figure 2b indicates that alkene insertion to form **^{5}V$_{1Pr}$** is irreversible, as the onward reaction via **^{5}TS(VI-VII)$_{1Pr}$**, is more accessible (by 6.9 kcal/mol) than the reverse β-H transfer to reform **^{5}IV$_{1Pr}$**. Similar patterns were computed for the alternative pathway involving the 2,1-migratory insertion of propene and the reaction of the resultant secondary metal-alkyl, LFe–^{i}Pr (**^{5}V$_{2Pr}$**), as well as for the analogous reactions with styrene (see ESI for full details). The regioselectivity of transfer hydrogenation can therefore be understood by considering the energies of the various migratory insertion transition states **TS(IV-V)**.

Computed free energies for the stationary points for the migratory insertions of propene and styrene with **^{5}III** are provided in Table 3. For propene a clear kinetic preference for 1,2-insertion to form LFe–^{n}Pr is seen, with **^{3}TS(IV-V)$_{1Pr}$** at 12.8 kcal/mol computed to be 2.9 kcal/mol more stable than **^{3}TS(IV-V)$_{2Pr}$**. Both quintet transition states are less accessible. This result is consistent with highly selective (> 90%) deuteration studies with a range of aliphatic alkenes in which reactions with DBpin and ^{n}BuND$_2$ label the internal and terminal positons respectively (*cf.* Scheme 2).

Table 3. Computed free energies (kcal/mol) of stationary points associated with the 1,2- and 2,1-migratory insertion of propene and styrene at LFe–H, **^{5}III**. Data are quoted relative to **^{5}III** and the free alkene.

Substrate / Selectivity	**^{5}IV$_R$**	**$^{3/5}$TS(IV-V)$_R$**	**^{5}V$_R$**
Propene (R = 1Pr) / 1,2	+7.3	+12.8 / +16.4	-11.4
Propene (R = 2Pr) / 2,1	+5.2	+15.7 / +18.1	-10.2
Styrene (R = 1St) / 1,2	+4.7	+12.6 / +15.8	-11.4
Styrene (R = 2St) / 2,1	+8.4	+14.5 / +11.7	-13.9

For styrene the experimental labelling studies indicate reaction via the primary metal alkyl (i.e. LFe–CH_2CH_2Ph, **V$_{1St}$**) is still favored, albeit with a reduced selectivity of around 75% (Scheme 2). This is reflected in a reduced difference of 1.9 kcal/mol between **^{3}TS(IV-V)$_{1St}$** and **^{3}TS(IV-V)$_{2St}$**. However, for the 2,1-insertion the quintet transition state, **^{5}TS(IV-V)$_{2St}$**, at 11.7 kcal/mol is now computed to be 0.9 kcal/mol more stable than **^{3}TS(IV-V)$_{1St}$**. This implies reaction via the secondary alkyl and hence a change in selectivity. Experimentally the precise selectivity is sensitive to electronic effects with, for example, the reaction of DBpin with 4-CF_3 styrene giving a 56:44 internal:terminal ratio. Moreover, the relative energies of these triplet and quintet transition states are very sensitive to the functional employed, and in particular the percentage of exact exchange. Reproducing precise selectivities is therefore challenging; however, based on our overall proposed mechanism, the observations that DBpin labels the internal position, and $PhND_2$ labels the terminal position clearly indicate these reactions proceed via the primary alkyl.[27,36,37]

4. Conclusions

In summary we have developed a remarkably simple yet rapid and mild method for the hydrogenation of alkenes using an amine and HBpin as the hydrogen sources. The chemistry tolerates a range of functional groups, is operational for both alkenes and alkynes, whilst 'internal' proton sources, for example aminoalkenes, can be employed. Hydroxyalkenes and alkynes can also undergo hydrogenation if the alcohol functionality is acidic. Selective mono-deuteration can be undertaken either at the terminal or internal position simply by varying the deuterating agent. Experimental observations and DFT calculations suggest that transfer hydrogenation reactions using ^{n}BuNH$_2$ and HBpin involve an oligomeric gel comprised of amine-borane adducts linked via intermolecular H-bonding. Calculations using an amine-borane dimer to model the transfer hydrogenation reagent for propene define a mechanism involving formation of an Fe-hydride active species, 1,2-insertion and rate-limiting protonolysis of the resultant primary alkyl. This mechanism is consistent with the observed deuteration regioselectivities with DBpin and $PhND_2$. The formation of the oligomeric gel is important in the chemoselectivity of this system as it serves to reduce the concentrations of both free HBpin and active N-H bonds, disfavoring the competing hydroboration and amine-borane dehydrocoupling reactions. It is also clear that this transfer hydrogenation system presents opportunities for expansion of the substrate scope, for both hydrogenation and deuteration, along with enantiocontrol and these are avenues we are currently investigating.

ASSOCIATED CONTENT

Supporting Information

Analysis data and NMR spectra for all products is provided in the supporting information (PDF file). A separate computational supporting information (PDF file) is also provided which contains all data relevant to the computational studies reported here, including methodology, benchmarking studies, energetics and coordinates of characterized stationary points. In addition a separate file (.xyz file) contains the coordinates of all the species discussed in this publication, readable by various molecular viewer programs. The Supporting Information is available free of charge on the ACS Publications website.

AUTHOR INFORMATION

Corresponding Author

* S.A.Macgregor@hw.ac.uk

* R.L.Webster@bath.ac.uk

Author Contributions

‡ MEV and NTC contributed equally.

Notes

The authors declare no competing financial interests.

ACKNOWLEDGMENT

The EPSRC is thanked for funding and the EPSRC UK National Mass Spectrometry Facility at Swansea University is thanked for mass spectrometry analyses.

REFERENCES

(1) a) Degraauw, C. F.; Peters, J. A.; Vanbekkum, H.; Huskens, J., Meerwein-Ponndorf-Verley Reductions and Oppenauer Oxidations - an Integrated Approach. *Synthesis-Stuttgart* **1994**, 1007; b) Corma, A.; Garcia, H., Lewis acids as catalysts in oxidation reactions: From homogeneous to heterogeneous systems. *Chem. Rev.* **2002**, *102*, 3837.

(2) a) Karvembu, R.; Prabhakaran, R.; Natarajan, K., Shvo's diruthenium complex: a robust catalyst. *Coord. Chem. Rev.* **2005**, *249*, 911; b) Conley, B. L.; Pennington-Boggio, M. K.; Boz, E.; Williams, T. J., Discovery, Applications, and Catalytic Mechanisms of Shvo's Catalyst. *Chem. Rev.* **2010**, *110*, 2294.

(3) a) Noyori, R.; Hashiguchi, S., Asymmetric transfer hydrogenation catalyzed by chiral ruthenium complexes. *Acc. Chem. Res.* **1997**, *30*, 97; b) Clapham, S. E.; Hadzovic, A.; Morris, R. H., Mechanisms of the H_2-hydrogenation and transfer hydrogenation of polar bonds catalyzed by ruthenium hydride complexes. *Coord. Chem. Rev.* **2004**, *248*, 2201; c) Wang, C.; Wu, X.; Xiao, J., Broader, Greener, and More Efficient: Recent Advances in Asymmetric Transfer Hydrogenation. *Chem. Asian J.* **2008**, *3*, 1750.

(4) a) Choi, J.; Tang, L.; Norton, J. R., Kinetics of Hydrogen Atom Transfer from $(\eta^5\text{-}C_5H_5)Cr(CO)_3H$ to Various Olefins: Influence of Olefin Structure. *J. Am. Chem. Soc.* **2007**, *129*, 234; b) Martin, N. J. A.; Ozores, L.; List, B., Organocatalytic Asymmetric Transfer Hydrogenation of Nitroolefins. *J. Am. Chem. Soc.* **2007**, *129*, 8976; c) Wang, J.; Song, G.; Peng, Y.; Zhu, Y., 3-Butyl-1-methylimidazolinium borohydride ([bmim][BH_4])—a novel reducing agent for the selective reduction of carbon–carbon double bonds in activated conjugated alkenes. *Tetrahedron Lett.* **2008**, *49*, 6518; d) Barrios-Francisco, R.; García, J. J., Semihydrogenation of alkynes in the presence of Ni(0) catalyst using ammonia-borane and sodium borohydride as hydrogen sources. *Appl. Catal. A.* **2010**, *385*, 108; e) Dong, H.; Berke, H., A mild and efficient rhenium-catalyzed transfer hydrogenation of terminal olefins using alcoholysis of amine–borane adducts as a reducing system. *J. Organomet. Chem.* **2011**, *696*, 1803; f) Nixon, T. D.; Whittlesey, M. K.; Williams, J. M. J., Ruthenium-catalysed transfer hydrogenation reactions with dimethylamine borane. *Tetrahedron Lett.* **2011**, *52*, 6652; g) Sumerin, V.; Chernichenko, K.; Nieger, M.; Leskelä, M.; Rieger, B.; Repo, T., Highly Active Metal-Free Catalysts for Hydrogenation of Unsaturated Nitrogen-Containing Compounds. *Adv. Synth. Catal.* **2011**, *353*, 2093; h) Hartmann, C. E.; Jurcik, V.; Songis, O.; Cazin, C. S. J., Tandem ammonia borane dehydrogenation/alkene hydrogenation mediated by [Pd(NHC)(PR_3)] (NHC = N-heterocyclic carbene) catalysts. *Chem. Commun.* **2013**, *49*, 1005; i) Erickson, K. A.; Stelmach, J. P. W.; Mucha, N. T.; Waterman, R., Zirconium-Catalyzed Amine Borane Dehydrocoupling and Transfer Hydrogenation. *Organometallics* **2015**, *34*, 4693; j) Pagano, J. K.; Stelmach, J. P. W.; Waterman, R., Cobalt-catalyzed ammonia borane dehydrocoupling and transfer hydrogenation under aerobic conditions. *Dalton Trans.* **2015**, *44*, 12074; k) Shao, Z.; Fu, S.; Wei, M.; Zhou, S.; Liu, Q., Mild and Selective Cobalt-Catalyzed Chemodivergent Transfer Hydrogenation of Nitriles. *Angew. Chem. Int. Ed.* **2016**, *55*, 14653; l) Zhou, Q.; Zhang, L.; Meng, W.; Feng, X.; Yang, J.; Du, H., Borane-Catalyzed Transfer Hydrogenations of Pyridines with Ammonia Borane. *Org. Lett.* **2016**, *18*, 5189; m) Korytiakova, E.; Thiel, N. O.; Pape, F.; Teichert, J. F., Copper(i)-catalysed transfer hydrogenations with ammonia borane. *Chem. Commun.* **2017**, *53*, 732.

(5) Yang, X.; Fox, T.; Berke, H., Facile metal free regioselective transfer hydrogenation of polarized olefins with ammonia borane. *Chem. Commun.* **2011**, *47*, 2053.

(6) Yang, X.; Zhao, L.; Fox, T.; Wang, Z.-X.; Berke, H., Transfer Hydrogenation of Imines with Ammonia–Borane: A Concerted Double-Hydrogen-Transfer Reaction. *Angew. Chem. Int. Ed.* **2010**, *49*, 2058.

(7) Zhou, Q.; Meng, W.; Yang, J.; Du, H., A Continuously Regenerable Chiral Ammonia Borane for Asymmetric Transfer Hydrogenations. *Angew. Chem. Int. Ed.* **2018**, *57*, 12111.

(8) Winner, L.; Ewing, W. C.; Geetharani, K.; Dellermann, T.; Jouppi, B.; Kupfer, T.; Schäfer, M.; Braunschweig, H., Spontaneous Metal-Free Transfer Hydrogenation of Iminoboranes with Ammonia Borane and Amine Boranes. *Angew. Chem. Int. Ed.* **2018**, *57*, 12275.

(9) Vogels, C. M.; Decken, A.; Westcott, S. A., Catalyzed hydroboration of nitrostyrenes and 4-vinylaniline: a mild and selective route to aniline derivatives containing boronate esters. *Tetrahedron Lett.* **2006**, *47*, 2419.

(10) Fu, S.; Chen, N.-Y.; Liu, X.; Shao, Z.; Luo, S.-P.; Liu, Q., Ligand-Controlled Cobalt-Catalyzed Transfer Hydrogenation of Alkynes: Stereodivergent Synthesis of *Z*- and *E*-Alkenes. *J. Am. Chem. Soc.* **2016**, *138*, 8588.

(11) Brzozowska, A.; Azofra, L. M.; Zubar, V.; Atodiresei, I.; Cavallo, L.; Rueping, M.; El-Sepelgy, O., Highly Chemo- and Stereoselective Transfer Semihydrogenation of Alkynes Catalyzed by a Stable, Well-Defined Manganese(II) Complex. *ACS Catal.* **2018**, *8*, 4103.

(12) Zhou, Y.-P.; Mo, Z.; Luecke, M.-P.; Driess, M., Stereoselective Transfer Semi-Hydrogenation of Alkynes to E-Olefins with N-Heterocyclic Silylene–Manganese Catalysts. *Chem. Eur. J.* **2018**, *24*, 4780.

(13) Espinal-Viguri, M.; Woof, C. R.; Webster, R. L., Iron-Catalyzed Hydroboration: Unlocking Reactivity through Ligand Modulation. *Chem. Eur. J.* **2016**, *22*, 11605.

(14) a) Espinal-Viguri, M.; King, A. K.; Lowe, J. P.; Mahon, M. F.; Webster, R. L., Hydrophosphination of Unactivated Alkenes and Alkynes Using Iron(II): Catalysis and Mechanistic Insight. *ACS Catal.* **2016**, *6*, 7892; b) King, A. K.; Gallagher, K. J.; Mahon, M. F.; Webster, R. L., Markovnikov versus anti-Markovnikov Hydrophosphination: Divergent Reactivity Using an Iron(II) β-Diketiminate Pre-Catalyst. *Chem. Eur. J.* **2017**, *23*, 9039.

(15) Coles, N. T.; Mahon, M. F.; Webster, R. L., Phosphine- and Amine-Borane Dehydrocoupling Using a Three-Coordinate Iron(II) β-Diketiminate Precatalyst. *Organometallics* **2017**, *36*, 2262.

(16) a) Langer, R.; Leitus, G.; Ben-David, Y.; Milstein, D., Efficient Hydrogenation of Ketones Catalyzed by an Iron

Pincer Complex. *Angew. Chem. Int. Ed.* **2011**, *50*, 2120; b) Yu, R. P.; Darmon, J. M.; Hoyt, J. M.; Margulieux, G. W.; Turner, Z. R.; Chirik, P. J., High-Activity Iron Catalysts for the Hydrogenation of Hindered, Unfunctionalized Alkenes. *ACS Catal.* **2012**, *2*, 1760; c) Fleischer, S.; Zhou, S.; Junge, K.; Beller, M., General and Highly Efficient Iron-Catalyzed Hydrogenation of Aldehydes, Ketones, and α,β-Unsaturated Aldehydes. *Angew. Chem. Int. Ed.* **2013**, *52*, 5120; d) Srimani, D.; Diskin-Posner, Y.; Ben-David, Y.; Milstein, D., Iron Pincer Complex Catalyzed, Environmentally Benign, E-Selective Semi-Hydrogenation of Alkynes. *Angew. Chem. Int. Ed.* **2013**, *52*, 14131; e) Hoyt, J. M.; Shevlin, M.; Margulieux, G. W.; Krska, S. W.; Tudge, M. T.; Chirik, P. J., Synthesis and Hydrogenation Activity of Iron Dialkyl Complexes with Chiral Bidentate Phosphines. *Organometallics* **2014**, *33*, 5781; f) Gieshoff, T. N.; Villa, M.; Welther, A.; Plois, M.; Chakraborty, U.; Wolf, R.; Jacobi von Wangelin, A., Iron-catalyzed olefin hydrogenation at 1 bar H_2 with a $FeCl_3$-$LiAlH_4$ catalyst. *Green Chem.* **2015**, *17*, 1408; g) Guo, N.; Hu, M.-Y.; Feng, Y.; Zhu, S.-F., Highly efficient and practical hydrogenation of olefins catalyzed by in situ generated iron complex catalysts. *Org. Chem. Front.* **2015**, *2*, 692; h) Xu, R.; Chakraborty, S.; Bellows, S. M.; Yuan, H.; Cundari, T. R.; Jones, W. D., Iron-Catalyzed Homogeneous Hydrogenation of Alkenes under Mild Conditions by a Stepwise, Bifunctional Mechanism. *ACS Catal.* **2016**, *6*, 2127; i) Büschelberger, P.; Gärtner, D.; Reyes-Rodriguez, E.; Kreyenschmidt, F.; Koszinowski, K.; Jacobi von Wangelin, A.; Wolf, R., Alkene Metalates as Hydrogenation Catalysts. *Chem. Eur. J.* **2017**, *23*, 3139; j) Murphy, L. J.; Ferguson, M. J.; McDonald, R.; Lumsden, M. D.; Turculet, L., Synthesis of Bis(phosphino)silyl Pincer-Supported Iron Hydrides for the Catalytic Hydrogenation of Alkenes. *Organometallics* **2018**, 10.1021/acs.organomet.8b00807; k) Sunada, Y.; Ogushi, H.; Yamamoto, T.; Uto, S.; Sawano, M.; Tahara, A.; Tanaka, H.; Shiota, Y.; Yoshizawa, K.; Nagashima, H., Disilaruthena- and Ferracyclic Complexes Containing Isocyanide Ligands as Effective Catalysts for Hydrogenation of Unfunctionalized Sterically Hindered Alkenes. *J. Am. Chem. Soc.* **2018**, *140*, 4119.

(17) Gärtner, D.; Welther, A.; Rad, B. R.; Wolf, R.; Jacobi von Wangelin, A., Heteroatom-Free Arene-Cobalt and Arene-Iron Catalysts for Hydrogenations. *Angew. Chem. Int. Ed.* **2014**, *53*, 3722.

(18) Trovitch, R. J.; Lobkovsky, E.; Bill, E.; Chirik, P. J., Functional group tolerance and substrate scope in bis(imino)pyridine iron catalyzed alkene hydrogenation. *Organometallics* **2008**, *27*, 1470.

(19) MacNair, A. J.; Tran, M.-M.; Nelson, J. E.; Sloan, G. U.; Ironmonger, A.; Thomas, S. P., Iron-catalysed, general and operationally simple formal hydrogenation using $Fe(OTf)_3$ and $NaBH_4$. *Org. Biomol. Chem.* **2014**, *12*, 5082.

(20) Morris, R. H., Mechanisms of the H_2- and transfer hydrogenation of polar bonds catalyzed by iron group hydrides. *Dalton Trans.* **2018**, *47*, 10809.

(21) a) Nishiguchi, T.; Fukuzumi, K., Homogeneous transfer-hydrogenation of olefins catalysed by Fe, Co, and Ni complexes: *o*- and *p*-dihydroxybenzene as hydrogen donors. *J. Chem. Soc. D. Chem. Commun.* **1971**, 139; b) Takeshi, N.; Kazuo, F., Transfer-hydrogenation and Transfer-hydrogenolysis. I. Transfer-hydrogenation of Cyclooctadienes Catalyzed by Dichlorobis(triphenylphosphine)iron(II). *Bull. Chem. Soc. Jpn.* **1972**, *45*, 1656; c) Wienhöfer, G.; Westerhaus, F. A.; Jagadeesh, R. V.; Junge, K.; Junge, H.; Beller, M., Selective iron-catalyzed transfer hydrogenation of terminal alkynes. *Chem. Commun.* **2012**, *48*, 4827.

(22) a) Enthaler, S.; Erre, G.; Tse, M. K.; Junge, K.; Beller, M., Biomimetic transfer hydrogenation of ketones with iron porphyrin catalysts. *Tetrahedron Lett.* **2006**, *47*, 8095; b) Enthaler, S.; Hagemann, B.; Erre, G.; Junge, K.; Beller, M., An Environmentally Benign Process for the Hydrogenation of Ketones with Homogeneous Iron Catalysts. *Chem. Asian J.* **2006**, *1*, 598; c) Enthaler, S.; Spilker, B.; Erre, G.; Junge, K.; Tse, M. K.; Beller, M., Biomimetic transfer hydrogenation of 2-alkoxy- and 2-aryloxyketones with iron–porphyrin catalysts. *Tetrahedron* **2008**, *64*, 3867; d) Gaillard, S.; Renaud, J.-L., Iron-Catalyzed Hydrogenation, Hydride Transfer, and Hydrosilylation: An Alternative to Precious-Metal Complexes? *ChemSusChem* **2008**, *1*, 505; e) Mikhailine, A.; Lough, A. J.; Morris, R. H., Efficient Asymmetric Transfer Hydrogenation of Ketones Catalyzed by an Iron Complex Containing a P-N-N-P Tetradentate Ligand Formed by Template Synthesis. *J. Am. Chem. Soc.* **2009**, *131*, 1394; f) Sonnenberg, J. F.; Coombs, N.; Dube, P. A.; Morris, R. H., Iron Nanoparticles Catalyzing the Asymmetric Transfer Hydrogenation of Ketones. *J. Am. Chem. Soc.* **2012**, *134*, 5893; g) Zuo, W.; Lough, A. J.; Li, Y. F.; Morris, R. H., Amine(imine)diphosphine Iron Catalysts for Asymmetric Transfer Hydrogenation of Ketones and Imines. *Science* **2013**, *342*, 1080; h) Kamitani, M.; Nishiguchi, Y.; Tada, R.; Itazaki, M.; Nakazawa, H., Synthesis of Fe–H/Si–H and Fe–H/Ge–H Bifunctional Complexes and Their Catalytic Hydrogenation Reactions toward Nonpolar Unsaturated Organic Molecules. *Organometallics* **2014**, *33*, 1532; i) Morris, R. H., Exploiting Metal-Ligand Bifunctional Reactions in the Design of Iron Asymmetric Hydrogenation Catalysts. *Acc. Chem. Res.* **2015**, *48*, 1494; j) Morris, R. H., Iron Group Hydrides in Noyori Bifunctional Catalysis. *The Chemical Record* **2016**, *16*, 2640.

(23) Lator, A.; Gaillard, S.; Poater, A.; Renaud, J.-L., Iron-Catalyzed Chemoselective Reduction of α,β-Unsaturated Ketones. *Chem. Eur. J.* **2018**, *24*, 5770.

(24) a) Bernoud, E.; Oulié, P.; Guillot, R.; Mellah, M.; Hannedouche, J., Well-Defined Four-Coordinate Iron(II) Complexes For Intramolecular Hydroamination of Primary Aliphatic Alkenylamines. *Angew. Chem. Int. Ed.* **2014**, *53*, 4930; b) Lepori, C.; Bernoud, E.; Guillot, R.; Tobisch, S.; Hannedouche, J., Experimental and computational mechanistic studies of the β-diketiminatoiron(II)-catalysed hydroamination of alkenes tethered to primary amines. *Chem. Eur. J.* **2018**, doi:10.1002/chem.201804681.

(25) ^{11}B NMR of the crude reaction mixture shows a small amount of competing hydroboration. For example, for the hydrogenation of allylbenzene using HBpin and $^nBuNH_2$ gives ~6% $Ph(CH_2)_3Bpin$, using $PhNH_2$ instead gives ~12% $Ph(CH_2)_3Bpin$ and $PhND_2$ gives ~8% $PhCH_2CHDCH_2Bpin$ (also see Scheme 2).

(26) a) Annby, U.; Gronowitz, S.; Hallberg, A., Reaction of the aromatic olefin 1-(1-hexenyl)-2-thiomethyl-benzene with $Cp_2Zr(H)Cl$. Unexpected cleavage of the methyl-sulphur bond. *J. Organomet. Chem.* **1989**, *368*, 295; b) Mizuta, T.; Sakaguchi, S.; Ishii, Y., Catalytic Reductive Alkylation of Secondary Amine with Aldehyde and Silane by an Iridium Compound. *J. Org. Chem.* **2005**, *70*, 2195.

(27) Vela, J.; Vaddadi, S.; Cundari, T. R.; Smith, J. M.; Gregory, E. A.; Lachicotte, R. J.; Flaschenriem, C. J.; Holland, P. L., Reversible Beta-Hydrogen Elimination of Three-Coordinate Iron(II) Alkyl Complexes: Mechanistic and Thermodynamic Studies. *Organometallics* **2004**, *23*, 5226.

(28) Bellows, S. M.; Cundari, T. R.; Holland, P. L., Spin Crossover during β-Hydride Elimination in High-Spin

Iron(II)– and Cobalt(II)–Alkyl Complexes. *Organometallics* **2013**, *32*, 4741.

(29) Moreover, hydrogenolysis of the putative LFe–^{n}Pr intermediate to form LFe–H and propane is computed to have a barrier of 28.3 kcal/mol.

(30) Romero, E. A.; Peltier, J. L.; Jazzar, R.; Bertrand, G., Catalyst-free dehydrocoupling of amines, alcohols, and thiols with pinacol borane and 9-borabicyclononane (9-BBN). *Chem. Commun.* **2016**, *52*, 10563.

(31) The structures of **AB2** and **AB4** reflect the importance of intramolecular hydrogen bonding involving the Bpin moiety. Calculations to locate an alternative form of **AB2** based on dihydrogen bonding suggest that such structures are not local minima.

(32) Grimme, S.; Schreiner, P. R., Computational Chemistry: The Fate of Current Methods and Future Challenges. *Angew. Chem. Int. Ed.* **2018**, *57*, 4170.

(33) Sun, Y.; Tang, H.; Chen, K.; Hu, L.; Yao, J.; Shaik, S.; Chen, H., Two-State Reactivity in Low-Valent Iron-Mediated C–H Activation and the Implications for Other First-Row Transition Metals. *J. Am. Chem. Soc.* **2016**, *138*, 3715.

(34) Harvey, J. N., Spin-forbidden reactions: computational insight into mechanisms and kinetics. *Wiley Interdisciplinary Reviews: Computational Molecular Science* **2013**, *4*, 1.

(35) Release of amino-borane from $\mathbf{AB2_{DHC}}$ has a computed ΔG of +0.6 kcal/mol, suggesting that this process, that will reveal a new layer of reactive amine-borane N-H bonds to engage in catalysis, should be accessible.

(36) Dias, R. P.; Prates, M. S. L.; De Almeida, W. B.; Rocha, W. R., DFT Study of the Ligand Effects on the Regioselectivity of the Insertion Reaction of Olefins in the Complexes $HRh(CO)_2(PR_3)(L)$ (R = H, F, Et, Ph, OEt, OPh, and L = Propene, Styrene). *Int. J. Quantum Chem* **2011**, *111*, 1280.

(37) We also examined the mechanism of transfer hydrogen of alkenes with aniline and HBpin. In this case no evidence for an amine-borane adduct was seen experimentally and no minimum corresponding to such a structure could be located computationally. Transfer hydrogenation is therefore likely to involve the free aniline and HBpin in this case. Protonolysis of the key LFe-propyl intermediate by aniline was computed to involve a transition state at +17.2 kcal/mol. This is significantly lower than the equivalent reaction with $^{n}BuNH_2$, (+21.2 kcal/mol, see Scheme 3) but remains less accessible than hydroboration with HBpin (+14.2 kcal/mol). Hydroboration is observed as a side reaction in the aniline/HBpin transfer hydrogen system (see Ref 25), however, the accessibility of this process is clearly over-estimated in the current model. This overall conclusion was not significantly affected by the choice of function (see ESI).

Insert Table of Contents artwork here

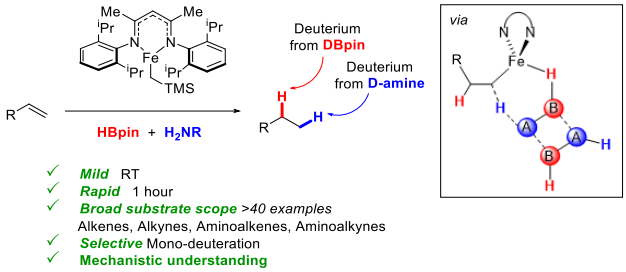

- ✓ ***Mild*** RT
- ✓ ***Rapid*** 1 hour
- ✓ ***Broad substrate scope*** *>40 examples*
  Alkenes, Alkynes, Aminoalkenes, Aminoalkynes
- ✓ ***Selective*** Mono-deuteration
- ✓ **Mechanistic understanding**